Spectral and Electrochemical Properties of the Diastereoisomeric Forms of Azobis(2-pyridine)-Bridged Diruthenium Species

Laurence S. Kelso, David A. Reitsma, and F. Richard Keene*

Department of Chemistry and Chemical Engineering, School of Molecular Sciences, James Cook University of North Queensland, Townsville, Queensland 4811, Australia

Received January 24, 1996[⊗]

A series of dinuclear complexes of ruthenium(II) have been synthesized in which α-azodiimines {such as azobis-(2-pyridine), apy, and azobis(4-methyl-2-pyridine), mapy} act as the bridge and 2,2′-bipyridine (bpy) or 4,4′-dimethyl-2,2′-bipyridine (Me_2bpy) as the terminal ligands. The diastereoisomeric forms of each species {ΔΛ *(meso)* and ΔΔ/ΛΛ *(rac)*} have been separated by cation-exchange chromatography and characterized by ^{1}H-NMR spectroscopy. Electronic spectral and electrochemical studies show there to be differences in inter-metal communication between the diastereoisomeric forms in each case. Comparison of the spectroelectrochemical behavior of the range of complexes has allowed unequivocal assignment of the site of the successive reduction processes observed in dinuclear complexes of this type.

Introduction

The stereoisomeric complexity of ligand-bridged polymetallic molecular assemblies based on tris(bidentate)metal centers has only recently been addressed.[1−6] The number of isomers in such species increases exponentially with nuclearity, and the consequences of this stereoisomerism may well prove significant in terms of intramolecular electron and energy transfer processes.

In the simplest case of a dinuclear species $[\{Ru(pp)_2\}_2(\mu\text{-}L)]^{4+}$ (where L is a symmetrical bridging ligand and pp is a bidentate terminal ligand), an examination of the two diastereoisomeric forms (Figure 1) shows a significant difference in the relative orientations of the terminal ligands "above" and "below" the plane of the bridging ligand. In the simplest case, where the bridging ligand is 2,2′-bipyrimidine,[1,4,6] or azobis-(2-pyridine) as in the present study, the "above plane" ligands are parallel in the ΔΔ/ΛΛ *(racemic)* and orthogonal in the ΔΛ/ΛΔ *(meso)* diastereoisomer.

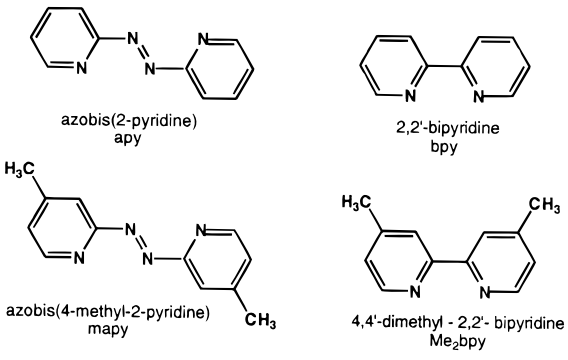

In addition to such stereochemical considerations, the bridging ligand affects the degree of metal−metal interaction in di- and oligonuclear complexes, as it determines the distance and relative orientation of the metal centers, and influences through-space electronic coupling and the degree of through-bond communication (via ligand−metal orbital overlap).[7,8]

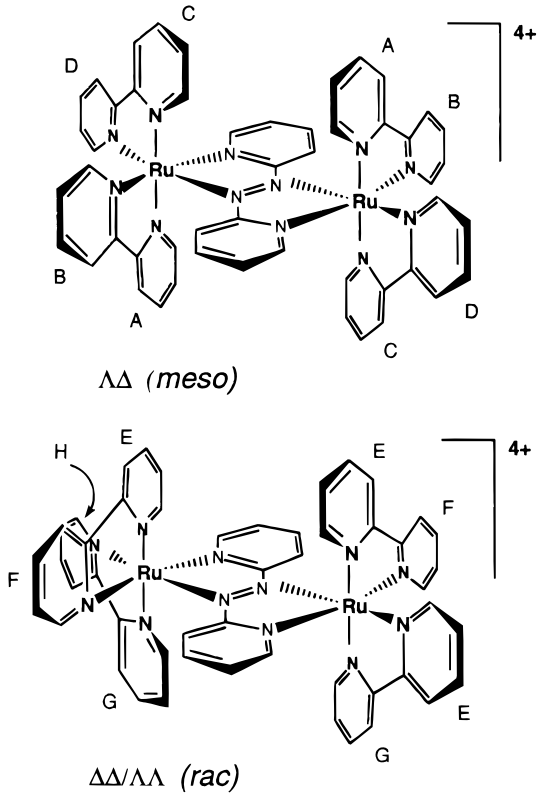

Figure 1. Diastereoisomeric forms (*meso* and *rac*) of $[\{Ru(bpy)_2\}_2(\mu\text{-apy})]^{4+}$ and ring-numbering scheme used for NMR discussion.

Ligands possessing the azo functionality have extremely low-lying π^* orbitals and are strongly π-accepting.[9−15] Moreover,

[⊗] Abstract published in *Advance ACS Abstracts,* August 1, 1996.

(1) Reitsma, D. A.; Keene, F. R. *J. Chem. Soc., Dalton Trans.* **1993**, 2859.
(2) Anderson, P. A.; Deacon, G. B.; Haarmann, K. H.; Keene, F. R.; Meyer, T. J.; Reitsma, D. A.; Skelton, B. W.; Strouse, G. F.; Thomas, N. C.; Treadway, J. A.; White, A. H. *Inorg. Chem.* **1995**, *34*, 6145.
(3) Rutherford, T. J.; Quagliotto, M. G.; Keene, F. R. *Inorg. Chem.* **1995**, *34*, 3857.
(4) Hua, X.; von Zelewsky, A. *Inorg. Chem.* **1991**, *30*, 3796.
(5) von Zelewsky, A. *Chimia* **1994**, *48*, 331.
(6) Hua, X.; von Zelewsky, A. *Inorg. Chem.* **1995**, *34*, 5791.
(7) Kalyanasundaram, K.; Nazeeruddin, M. K. *Inorg. Chim. Acta* **1994**, *226*, 213.
(8) Balzani, V.; Scandola, F. *Supramolecular Photochemistry*; Ellis Horwood: Chichester, U.K., 1991; p 427.
(9) Ernst, S. D.; Kaim, W. *Inorg. Chem.* **1989**, *28*, 1520.
(10) Krause, R. A.; Krause, K. *Inorg. Chem.* **1980**, *19*, 2600.
(11) Krause, R. A.; Krause, K. *Inorg. Chem.* **1982**, *21*, 1714.
(12) Krause, R. A.; Krause, K. *Inorg. Chem.* **1984**, *23*, 2195.

S0020-1669(96)00089-4 CCC: $12.00

dinuclear complexes in which ligands such as azobis(2-pyridine) function as the bridge have comproportionation constants (K_c) in excess of 10^8 for the diruthenium case and hence exhibit a very high degree of metal−metal interaction.[7,9,13,16,17] Bridging ligands of this type also are found to enhance the structural differences between the diastereoisomers of such dinuclear species.

Despite the intense interest in dimetallic polypyridyl complexes, studies of their properties have been based almost exclusively on nonseparated isomeric mixtures so that reported data may be thought of as an average of the contributions of each form. The high degree of metal−metal interaction within α-azodiimine-bridged dinuclear complexes, coupled with structural dissimilarities between the diastereoisomeric pairs, prompted an examination of the spectral and electrochemical behavior of the different forms. By subtle variation of the bridge via incorporation of ring substituents (e.g. methyl groups) the electronic character of the resulting complexes may be probed. The photophysical and electrochemical effects of variations in the terminal (nonbridging) ligands upon the bridge also warrant examination[18] and may be probed in a similar manner.

In the present work, we describe the synthesis of a series of mono- and dinuclear complexes containing α-azodiimine ligands such as azobis(2-pyridine) and azobis(4-methyl-2-pyridine) {abbreviated apy and mapy, respectively} and assess the influence of the bridge on metal−metal and also metal−ligand interactions. Significantly, differences in various properties of the separated diastereoisomers of α-azodiimine-bridged dinuclear ruthenium(II) complexes are observed.

Experimental Section

Physical Measurements. Electronic spectra were recorded using a Cary 5E UV−vis−near-IR spectrophotometer. NMR spectra were recorded on a Bruker Aspect AM3000 spectrometer. Electrochemical measurements were made in a Vacuum Atmospheres drybox (Ar) using a Bioanalytical Systems (BAS) 100A electrochemical analyzer. Cyclic and differential pulse voltammetries were carried out in a three-electrode cell using a platinum microdisk working electrode, with a platinum counter electrode. All potentials are quoted relative to an $Ag/AgNO_3$ reference electrode (0.01 M in CH_3CN), which is 0.095 V cathodic of the ferrocene/ferrocenium couple as an internal standard. Elemental analyses were performed within the School of Molecular Sciences, JCUNQ. The successive oxidized and reduced forms of the dinuclear species were selectively generated and characterized *in situ* by electronic absorption spectroscopy using a cryostatic optically transparent thin-layer electrochemical (OTTLE) cell[19] in conjuction with a Perkin-Elmer Lambda 9 UV−vis−near-IR spectrophotometer.

Materials. 2-Aminopyridine, sodium toluene-4-sulfonate, sodium ditoluoyl-(+)-tartrate, 2,2′-bipyridine, 4,4′-dimethyl-2,2′-bipyridine (all Adrich), 2-amino-4-methylpyridine (Fluka), $RuCl_3 \cdot 3H_2O$ (Strem), and commercial grade NaOCl (12.5% w/v, Swimfree pool chlorine) were used as supplied. The electrolyte tetra-*n*-butylammonium perchlorate {$[(n\text{-}C_4H_9)_4N]ClO_4$; purum, Fluka) was recrystallized from ethyl acetate/hexane and dried at 60 °C under vacuum. Spectral grade acetonitrile (Sigma) was used for all spectroscopic and electrochemical measurements. All other reagent grade solvents were used without further purification.

Ligand Syntheses. Azobis(2-pyridine), **apy**, was prepared by modification of literature methods.[20,21] The crude product was purified by vacuum chromatography on silica gel,[22] using dichloromethane as eluent. Unreacted starting material eluted first, followed by the highly colored major product band. Red needles were obtained after recrystallization from petroleum ether (600 cm^3, bp 60−80 °C). Yield: 3.82 g (35%). Mp: 84.5−85 °C (lit.[23] 85−86 °C). ^{1}H-NMR (CD_3CN): δ 8.74 ($H^{6,6'}$, d), 8.00 ($H^{4,4'}$, dd), 7.80 ($H^{3,3'}$, d), 7.64 ($H^{5,5'}$, dd). The ^{1}H-NMR spectrum in $CDCl_3$ was consistent with a literature report.[13]

Azobis(4-methyl-2-pyridine), mapy. A rapidly stirred solution of sodium hypochlorite (500 cm^3, 12.5% w/v) was chilled in an acetone/dry ice slush bath until solids began to precipitate. To this was added (all at once) a solution of 2-amino-4-methylpyridine {12.1 g in 1:1 CH_3CN/H_2O (120 cm^3)}. Stirring and cooling were continued for 4 min, after which the resulting orange solution was extracted rapidly with diethyl ether (4 × 100 cm^3). Between each extraction, the remaining aqueous layer was rechilled, since the continuing reaction of unreacted starting material with hypochlorite ion is exothermic. The organic layers were combined and dried over anhydrous Na_2SO_4, and the solvent was removed to give an orange solid. The crude product was purified as for apy. An orange crystalline product was obtained after two recrystallizations from petroleum ether (600 cm^3, bp 60−80 °C). Yield 3.44 g (29%). Mp: 143.5−145 °C (lit.[23] 149−151 °C). ^{1}H-NMR ($CDCl_3$): δ 8.62 ($H^{6,6'}$, d), 7.82 ($H^{3,3'}$, d), 7.27 ($H^{5,5'}$, dd), 2.46 (CH_3, s). Anal. Calcd for $C_{12}H_{12}N_4$: C, 67.9; H, 5.70; N, 26.4. Found: C, 67.3; H, 5.67; N, 26.2.

$[Ru(pp)_2L]^{2+}$ (II). Mononuclear complexes were prepared from the appropriate $[Ru(pp)_2Cl_2]$ precursor[24] and an excess of the bridging α-azodiimine.[25] In a typical reaction, $[Ru(Me_2bpy)_2Cl_2]$ (500 mg; 0.925 mmol) and apy (511 mg; 2.77 mmol) were refluxed in 50% aqueous methanol (50 cm^3) for 1h under N_2. The solvent was removed, and the solids were redissolved in methanol (5 cm^3) for purification via gel permeation chromatography using a column of Sephadex LH-20 as support and methanol as eluent. The major claret-red product band eluted first, followed by a red-orange band of apy. The product band was evaporated to dryness, the residue redissolved in water, the solution filtered to remove any remaining solids, and the filtrate diluted to a total volume of 150 cm^3. Saturated aqueous KPF_6 solution (8 cm^3) was added dropwise to the stirred solution, and the precipitated hexafluorophosphate salt was collected via vacuum filtration, washed with diethyl ether, and air-dried. Recrystallization was achieved from acetone/diethyl ether. $[Ru(apy)(bpy)_2](PF_6)_2 \cdot C_3H_6O$: yield 210 mg (51%). Anal. Calcd for $RuC_{33}H_{30}N_8OP_2F_{12}$: C, 41.9; H, 3.20; N, 11.9. Found: C, 41.5; H, 2.87; N, 12.0. ^{1}H-NMR (CD_3CN): δ 8.58, 8.54, 8.40, 8.26 (H^3_{bpy}, d), 8.19, 8.12, 8.15, 7.94 (H^4_{bpy}, dd), 7.52, 7.48, 7.47, 7.25 (H^5_{bpy}, dd), 7.48, 8.03, 7.26, 7.52 (H^6_{bpy}, d), 8.85, 7.52 (H^3_{apy}, d), 8.24, 7.87 (H^4_{apy}, dd), 7.67, 7.35 (H^5_{apy}, dd), 7.88, 7.89 (H^6_{apy}, d). $[Ru(apy)(Me_2bpy)_2](PF_6)_2$: yield 525 mg (60%). Anal. Calcd for $RuC_{34}H_{32}N_8P_2F_{12}$: C, 43.3; H, 3.42; N, 11.9. Found: C, 43.8; H, 3.27; N, 11.7. ^{1}H-NMR (CD_3CN): δ 8.43, 8.35, 8.24, 8.09 ($H^3_{Me_2bpy}$, s), 2.57, 2.52, 2.54, 2.44 (CH_{3Me_2bpy}, s), 7.37, 7.28, 7.27, 7.05 ($H^5_{Me_2bpy}$, d), 7.28, 7.78, 7.05, 7.28 ($H^6_{Me_2bpy}$, d), 8.79, 7.51 (H^3_{apy}, d), 8.20, 7.85 (H^4_{apy}, dd), 7.65, 7.33 (H^5_{apy}, dd), 7.86, 7.92 (H^6_{apy}, d). $[Ru(mapy)(bpy)_2](PF_6)_2 \cdot 0.5C_3H_6O$: yield 388 mg (91%). Anal. Calcd for $RuC_{33.5}H_{31}N_8O_{0.5}P_2F_{12}$: C, 42.3; H, 3.28; N, 11.8. Found: C, 42.9; H, 3.06; N, 12.0. ^{1}H-NMR (CD_3CN): δ 8.57, 8.51, 8.40, 8.24 (H^3_{bpy}, d), 8.18, 8.11, 8.16, 7.92 (H^4_{bpy}, dd), 7.57, 7.57, 7.47, 7.22 (H^5_{bpy}, dd), 7.48, 8.06, 7.27, 7.50 (H^6_{bpy}, d), 8.68, 7.31 (H^3_{mapy}, d), 2.86, 2.33 (CH_{3mapy}, s), 7.49, 7.15 (H^5_{mapy}, dd), 7.69, 7.74 (H^6_{mapy}, d). $[Ru(mapy)(Me_2bpy)_2](PF_6)_2$: yield 350 mg (78%). Anal. Calcd for $RuC_{36}H_{36}N_8P_2F_{12}$: C, 44.5; H, 3.73; N, 11.5. Found: C, 45.1; H, 3.58; N, 11.2. ^{1}H-NMR (CD_3CN): δ 8.42, 8.35, 8.24, 8.09 ($H^3_{Me_2bpy}$, s), 2.57, 2.52, 2.54, 2.43 (CH_{3Me_2bpy}, s), 7.36, 7.27, 7.26, 7.03 ($H^5_{Me_2bpy}$,

(13) Krejcik, M.; Zalis, S.; Klima, J.; Sykora, D.; Matheis, W.; Klein, A.; Kaim, W. *Inorg. Chem.* **1993**, *32*, 3362.
(14) Goswami, S.; Chakravarty, A. R.; Chakravorty, A. *Inorg. Chem.* **1982**, *21*, 2737.
(15) Bessel, C. A.; Margarucci, J. A.; Acquaye, J. H.; Rubino, R. S.; Crandall, J.; Jircitano, A. J.; Takeuchi, K. J. *Inorg. Chem.* **1993**, *32*, 5779.
(16) Ernst, S.; Kasack, V.; Kaim, W. *Inorg. Chem.* **1988**, *27*, 1146.
(17) Kaim, W.; Kohlmann, S. *Inorg. Chem.* **1987**, *26*, 68.
(18) Giuffrida, G.; Campagna, S. *Coord. Chem. Rev.* **1994**, *135*, 517.
(19) Duff, C. M.; Heath, G. A. *Inorg. Chem.* **1991**, *30*, 2528.
(20) Kirpal, A.; Reiter, L. *Chem. Ber.* **1927**, *60*, 664.
(21) Baldwin, D. A.; Lever, A. B. P.; Parish, R. V. *Inorg. Chem.* **1969**, *8*, 107.
(22) Coll, J. C.; Bowden, B. F. *J. Nat. Prod.* **1986**, *49*, 934.
(23) Campbell, N.; Henderson, A. W.; Taylor, D. *J. Chem. Soc.* **1953**, 1281.
(24) Togano, T.; Nagao, N.; Tsuchida, M.; Kumakura, H.; Hisamatsu, K.; Howell, F. S.; Mukaida, M. *Inorg. Chim. Acta* **1992**, *195*, 221.
(25) Brown, G. M.; Weaver, T. R.; Keene, F. R.; Meyer, T. J. *Inorg. Chem.* **1976**, *15*, 190.

d), 7.26, 7.83, 7.05, 7.26 ($H^6_{Me_2bpy}$, d), 8.65, 7.36 (H^3_{mapy}, d), 2.67, 2.32 (CH_{3mapy}, s), 7.49, 7.13 (H^5_{mapy}, dd), 7.67, 7.76 (H^6_{mapy}, d).

$[\{Ru(pp)_2\}_2(\mu\text{-}L)]^{4+}$ (III). Typically, 1 mol equiv of $[Ru(pp)_2Cl_2]$ and 1.5 mol equiv of $[Ru(pp)_2L]^{2+}$ were dissolved in a 50% aqueous methanol solution under N_2. The mixture was refluxed for at least 5 days. $AgNO_3$ (2 mol equiv) and $[Ru(pp)_2Cl_2]$ (1 mol equiv) were added to the solution each day. The mixture was filtered (Celite) and the filtrate concentrated on a rotary evaporator. Purification was achieved by cation-exchange chromatography (SP-Sephadex C-25; eluent 0.5 M NaCl). Separation of the diastereoisomers and resolution of the *rac* forms were achieved by cation-exhange chromatography on the same support using 0.25 M sodium toluene-4-sulfonate and 0.25 M sodium ditoluoyl-(+)-tartrate solutions as eluents, respectively.[1,3] The product was precipitated as the PF_6^- salt by addition of a saturated solution of KPF_6 to the green eluent. The green solid was collected and washed with a dilute KPF_6 solution. $[\{Ru(bpy)_2\}_2(\mu\text{-apy})](PF_6)_4$: yield 52%. $[\{Ru(Me_2bpy)_2\}_2(\mu\text{-apy})](PF_6)_4$: yield 41%. $[\{Ru(bpy)_2\}_2(\mu\text{-mapy})](PF_6)_4$: yield 40%, isomer ratio *meso:rac* = 3.8:1. $[\{Ru(Me_2bpy)_2\}_2(\mu\text{-mapy})](PF_6)_4$: yield 90%. $[(bpy)_2Ru(\mu\text{-mapy})Ru(Me_2bpy)_2](PF_6)_4$: yield 79%, isomer ratio *meso:rac* = 1.67:1.

Microanalytical data are provided for the two diastereiosomeric forms of one dinuclear species, $[\{Ru(Me_2bpy)_2\}_2)(\mu\text{-apy})](PF_6)_4$, by way of an example. Anal. Calcd for *meso*-$[\{Ru(Me_2bpy)_2\}_2)(\mu\text{-apy})](PF_6)_4$, $Ru_2C_{58}H_{56}N_{12}P_4F_{24}$: C, 40.9; H, 3.31; N, 9.8. Found: C, 41.3; H, 3.08; N, 9.4. Anal. Calcd for *rac*-$[\{Ru(Me_2bpy)_2\}_2)(\mu\text{-apy})](PF_6)_4\cdot 2H_2O$, $Ru_2C_{58}H_{60}N_{12}O_2P_4F_{24}$: C, 40.0; H, 3.48; N, 9.6. Found: C, 39.8; H, 3.11; N, 9.2. In general, characterization of dinuclear species was achieved using ^{1}H-NMR and electrochemical techniques (see Results and Discussion), as microanalyses are not particularly discriminating for larger molecules.

Results and Discussion

Syntheses. The α-azodiimine ligands apy and mapy were obtained by oxidation of 2-aminopyridine and 2-amino-4-methylpyridine, respectively, in sodium hypochlorite solution. The *trans* isomer is thermodynamically preferred,[13,23] and after purification there was no evidence from ^{1}H-NMR studies of any of the *cis* form being present.

The reaction between $[Ru(pp)_2Cl_2]$ (pp = bpy or Me_2bpy) and excess L (L = apy or mapy) proceeds at reflux in 50% aqueous methanol. Mononuclear complexes of the form $[Ru(pp)_2L]^{2+}$ were isolated as hexafluorophosphate salts and were used as precursors in the synthesis of dinuclear species.

The dinuclear complexes were generally prepared by the reaction of excess $[Ru(pp)_2Cl_2]$ with $[Ru(pp)_2L]^{2+}$ in aqueous methanol in the presence of Ag^+. The attachment of the second metal center to the bridging ligand (to give $[(pp)_2Ru(\mu\text{-}L)Ru(pp)_2]^{4+}$) is not a facile step, and the typical synthesis required days of refluxing and periodic additions of both excess $[Ru(pp)_2Cl_2]$ and $AgNO_3$. The large activation barrier to the formation of apy-bridged dimers from monomeric precursors has previously been attributed to steric interactions between the 6- and 6′-protons of the bridge and the coordinating nitrogen atoms of adjacent ligands.[9,17] The azobis(2-pyridine) bridging ligands are exceptions to the "charge transfer assisted polynucleation" phenomenon, in which dimer formation is facilitated.[9,17,26] All attempts to prepare the dinuclear complexes directly from the bridging ligand and a stoichiometric excess of $[Ru(pp)_2Cl_2]$ gave diminished yields compared with the two-step route. Previous work partially addressed these synthetic difficulties by the use of higher boiling solvents (1-butanol) and extended reaction times.[16]

Separation of Diastereoisomeric Pairs. We have previously shown that the diastereoisomeric pairs of ligand-bridged dinuclear polypyridyl compounds may be separated by cation-exchange chromatography.[1] By use of this chromatographic technique, the diastereoisomers of all five dinuclear compounds were separated within a 20 cm column length, considerably less than the column length required for the separation of compounds in which 2,2′-bipyrimidine (bpm) and 2,3-bis(2-pyridyl)pyrazine (dpp) were the bridging ligands.[1]

The relative ease of separation may be rationalized in terms of the stereochemistry. As described above, the diastereoisomers differ in terms of the relative orientation of the terminal ligands.[1,4,6,27] In the case where the bridging ligand is an α-azodiimine (rather than bpm or dpp), the differences are even more pronounced, as the offset position of the metal centers places the "above plane" ligands almost coplanar in the ΔΔ/ΛΛ *(rac)* isomer (Figure S1, Supporting Information).

An interesting observation during the separation was the noticeable difference in the color of the diastereoisomers on the column. The first band was dark green and the second band olive green for all five dinuclear compounds.

Most of the dinuclear compounds investigated were found to have only a slight diastereoisomeric excess favoring the *meso* form, which was eluted first. However, for the complex $[\{Ru(bpy)_2\}_2(\mu\text{-mapy})]^{4+}$ the isomer ratio (assessed by ^{1}H-NMR integration) was 3.8:1. A preference for the *meso* diastereoisomer would be predicted on stereochemical grounds, as examination of models reveals possible inter-ligand interactions in the *rac* form.

Previous studies of α-azodiimine-bridged dinuclear compounds suggested that only one diastereoisomer is observed.[13] The current work clearly shows the presence of both isomers. In the previous studies, the reactions were performed at higher temperatures and it is possible that under such conditions one isomer may dominate. Additionally, the purification techniques used previously may have excluded one isomer due to the differences in solubilities of the diastereoisomeric forms.

Resolution of *rac* (ΔΔ/ΛΛ)-$[\{Ru(Me_2bpy)\}_2(\mu\text{-apy})]^{4+}$. The four "symmetrical" dinuclear compounds prepared in this study (i.e. those with the same terminal ligands on both metal centers) have two diastereoisomers, one *racemic* (consisting of the ΔΔ/ΛΛ enantiomeric pairs) and the other a *meso* (ΔΛ) form. Consequently, the resolution of one of the diastereoisomers would unequivocally establish its identity as *rac*. We have developed chromatographic methods for separation of enantiomers by ion-exchange chromatography, using chiral eluents.[3,28] Resolution of the species corresponding to band 1 and band 2 of $[\{Ru(Me_2bpy)\}_2(\mu\text{-apy})]^{4+}$ from the separation of the diastereoisomers was attempted by cation-exchange chromatography using an aqueous solution of sodium toluoyl-(+)-tartrate as the eluent. Band 2 was found to separate into two bands—the isolated cations of which had equal and opposite ORD curves—allowing the assignment of band 2 as the *rac* form. The ^{1}H-NMR studies described below are consistent with this assertion.

^{1}H-NMR Studies. The ^{1}H-NMR data for the mononuclear and dinuclear compounds are listed in Table 1. The notation used for the pyridine rings in the terminal ligands of the two diastereoisomeric forms is shown in Figure 1.

In each case, the H^3 to H^6 protons of each pyridyl ring show the normal coupling patterns,[29,30] and assignments were made on the basis of COSY spectra (an example is given in Figure 2

(26) Kohlmann, S.; Ernst, S.; Kaim, W. *Angew. Chem., Int. Ed. Engl.* **1985**, *24*, 684.

(27) Hage, R.; Dijkhuis, A. H. J.; Haasnoot, J. G.; Prins, R.; Reedjik, J.; Buchanan, B. E.; Vos, J. G. *Inorg. Chem.* **1988**, *27*, 2185.

(28) Reitsma, D. A.; Keene, F. R. Manuscript in preparation.

(29) Bolger, J. A.; Ferguson, G.; James, J. P.; Long, C.; McArdle, P.; Vos, J. G. *J. Chem. Soc., Dalton Trans.* **1993**, 1577.

(30) Orellana, G.; Ibarra, C. A.; Santoro, J. *Inorg. Chem.* **1988**, *27*, 1025.

Table 1. 300 MHz ^{1}H-NMR Data[a] for the Dinuclear Complexes Used in This Study (PF_6^- Salts; CD_3CN Solvent)

		[{Ru(bpy)$_2$}$_2$-(μ-apy)]$^{4+}$	[{Ru(bpy)$_2$}$_2$-(μ-mapy)]$^{4+}$	[{Ru(Me$_2$bpy)$_2$}$_2$-(μ-apy)]$^{4+}$	[{Ru(Me$_2$bpy)$_2$}$_2$-(μ-mapy)]$^{4+}$	[Ru(bpy)$_2$(μ-mapy)-Ru(Me$_2$bpy)$_2$]$^{4+}$ [c]	
						bpy	Me$_2$bpy
				$\Delta\Lambda$ Diastereoisomers			
ring A	H^3	8.57	8.50	8.38	8.35	8.51	8.36
	H^4 [b]	8.28	8.22	2.58	2.58	8.23	2.59
	H^5	7.72	7.69	7.46	7.47	7.69	7.46
	H^6	7.21	7.16	7.03	6.99	7.20	6.94
ring B	H^3	8.59	8.55	8.40	8.41	8.55	8.42
	H^4 [b]	8.27	8.22	2.58	2.58	8.22	2.59
	H^5	7.63	7.62	7.39	7.42	7.61	7.43
	H^6	7.83	7.83	7.50	7.57	7.83	7.57
ring C	H^3	8.64	8.60	8.42	8.43	8.60	8.45
	H^4 [b]	8.28	8.22	2.58	2.58	8.20	2.59
	H^5	7.57	7.51	7.36	7.34	7.50	7.35
	H^6	7.49	7.47	7.24	7.27	7.50	7.26
ring D	H^3	8.57	8.53	8.36	8.37	8.54	8.38
	H^4 [b]	8.16	8.11	2.51	2.52	8.12	2.51
	H^5	7.24	7.21	6.97	6.99	7.18	7.01
	H^6	7.24	7.16	6.92	6.93	7.18	6.90
azodiimine	H^3	8.06	7.74	8.00	7.71	7.72, 7.72	
	H^4 [b]	7.77	2.06	7.70	2.06	2.06, 2.06	
	H^5	7.66	7.44	7.60	7.43	7.43, 7.43	
	H^6	7.88	7.62	7.80	7.61	7.61, 7.61	
				$\Delta\Delta/\Lambda\Lambda$ Diastereoisomers			
ring E	H^3	8.45	8.42	8.28	8.29	8.42	8.26
	H^4 [b]	8.12	8.09	2.56	2.58	8.07	2.58
	H^5	6.90	6.86	6.65	6.68	6.87	6.65
	H^6	6.38	6.33	6.22	6.11	6.39	6.06
ring F	H^3	8.50	8.48	8.31	8.34	8.48	8.32
	H^4 [b]	8.21	8.18	2.56	2.57	8.18	2.56
	H^5	7.63	7.60	7.40	7.42	7.60	7.43
	H^6	7.84	7.86	7.56	7.62	7.88	7.62
ring G	H^3	8.76	8.69	8.54	8.52	8.68	8.54
	H^4 [b]	8.30	8.22	2.59	2.58	8.22	2.58
	H^5	7.42	7.39	7.18	7.20	7.40	7.20
	H^6	7.68	7.63	7.38	7.38	7.62	7.38
ring H	H^3	8.76	8.69	8.54	8.52	8.68	8.54
	H^4 [b]	8.28	8.23	2.59	2.58	8.21	2.58
	H^5	7.48	7.41	7.27	7.26	7.40	7.27
	H^6	7.10	7.09	6.84	6.88	7.08	6.86
azodiimine	H^3	8.36	8.05	8.29	8.02	8.05, 8.03	
	H^4 [b]	7.89	2.18	7.80	2.15	2.18, 2.18	
	H^5	7.68	7.46	7.61	7.42	7.45, 7.43	
	H^6	7.89	7.63	7.81	7.59	7.62, 7.62	

[a] For ring designation, see Figure 3. H^3 is a doublet (d) and a singlet (s) when the terminal ligand is bpy and Me$_2$bpy, respectively; H^4 is dd (bpy) or s (i.e. CH_3; Me$_2$bpy); H^5 is dd (bpy) or d (Me$_2$bpy); H^6 is d in both cases. Coupling constants (Hz): $J_{3-4} = 8$, $J_{4-5} = 8$, $J_{5-6} = 5$, $J_{3-5} = 1.2$, $J_{4-6} = 1.2$. [b] For the methyl-substituted pyridyl rings the methyl instead of the H^4 chemical shift is indicated. [c] $\Delta\Lambda$ and $\Lambda\Delta$ enantiomers.

for the species $\Delta\Lambda/\Lambda\Delta$-[(Me$_2$bpy)$_2$Ru($\mu$-mapy)Ru(bpy)$_2$]$^{4+}$) and selective ^{1}H-decoupling experiments. In the case where methyl-substituted pyridyl rings were present (Me$_2$bpy and mapy), the chemical shift of the methyl singlet is provided in Table 1 in place of the H^4 signal. The connectivity between the two pyridyl rings of each ligand was established by NOE experiments. The H^3 protons show an NOE to the adjacent H^3 proton on the connected pyridyl ring of the same ligand. For example, in the complex *rac*-[{Ru(Me$_2$bpy)$_2$}$_2$(μ-mapy)]$^{4+}$ the H^3 proton of ring A shows an NOE to H^3 on ring B and H^3 on ring C shows an NOE to H^3 on ring D (Figure S2, Supporting Information). Connectivity was established for the *meso* ($\Delta\Lambda$) dimers in an analogous manner.

For the mononuclear compounds, there are six distinguishable pyridyl rings. The coordinated apy (or mapy) ligand is unsymmetrical, and hence there are four bpy (or Me$_2$bpy) pyridyl environments and two apy (or mapy) pyridyl environments. In the dinuclear complexes in which the two metal centers have the same terminal ligands, the *racemic* form ($\Delta\Delta/\Lambda\Lambda$) has C_2 and the *meso* form ($\Delta\Lambda$) has C_i point group symmetry—accordingly both species show five pyridyl environments. On the other hand, both diastereoisomers of the "mixed" [(bpy)$_2$Ru(μ-mapy)Ru(Me$_2$bpy)$_2$]$^{4+}$ species have 10 pyridyl environments.

The most notable aspect of the ^{1}H-NMR spectroscopic studies is the difference in the spectra between the diastereoisomeric pairs of each dinuclear species. As an example, the spectra for the complex [{Ru(Me$_2$bpy)$_2$}$_2$(μ-mapy)]$^{4+}$ are given in Figure 3. The *meso* isomer of all five dimers have similar spectra (allowing for the 0.2−0.3 ppm upfield shift of protons adjacent to a methyl group and the different coupling pattern of the methyl-substituted pyridyls). Likewise, the spectra of the *rac* isomers are also similar. It is apparent that the ligand geometry has a greater effect on chemical shift than methyl substitution.

In the dinuclear species, the assignment of the resonances associated with individual terminal ligands is based on the

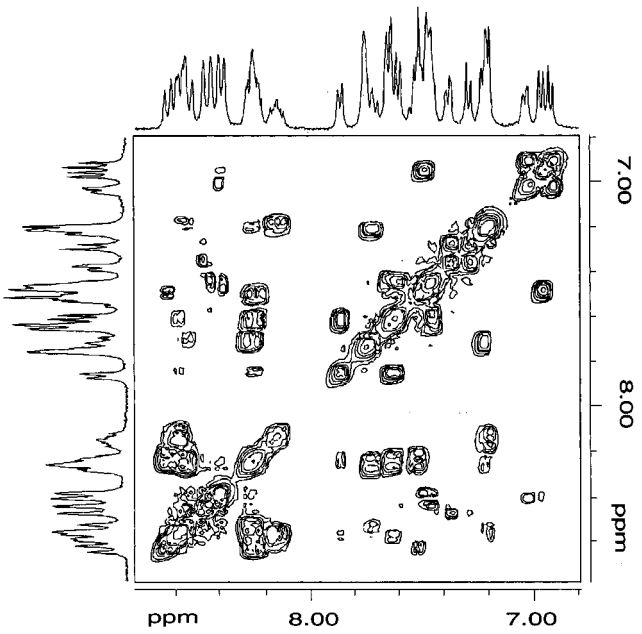

Figure 2. COSY ^{1}H-NMR spectrum for $\Delta\Lambda/\Lambda\Delta$-[(bpy)$_2$Ru($\mu$-mapy)-Ru(Me$_2$bpy)$_2$]$^{4+}$ (300 MHz in CD_3CN).

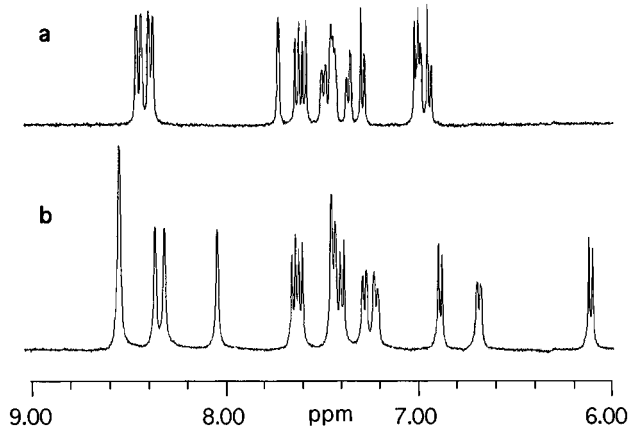

Figure 3. 300 MHz ^{1}H-NMR spectra (CD_3CN) of diastereoisomers of [{Ru(Me$_2$bpy)$_2$}$_2$(μ-mapy)]$^{4+}$: (a) *meso* ($\Delta\Lambda$); (b) *rac* ($\Delta\Delta/\Lambda\Lambda$).

differential ring current effect of the two ligands above (or below) the plane of the bridge between the two diastereoisomers (refer to Figure 1). There are four environments for the H^6 protons of the terminal ligands, two over the bridge and two directed away from it. The H^6 protons over the bridge will show the greatest change in chemical shift between the two isomers. In one environment the H^6 protons (of rings A and E) are positioned over the apy (or mapy) pyridyl rings and in the other "over bridge" environment the H^6 protons (of rings C and G) are over the azo moiety. For the complex [{Ru(Me$_2$-bpy)$_2$}$_2$(μ-apy)]$^{4+}$ the H^6 proton of ring E is 0.9 ppm upfield of the H^6 proton of ring A and the H^6 proton of ring G is 0.14 ppm downfield of the same proton in ring C. Examination of models reveals that the H^6 proton on ring E lies directly over the pyridyl ring of the ligand positioned across the bridge (the other ring E; see Figure 1) and is in a considerably shielded environment compared to the H^6 proton on ring A, which is directly in the plane of the pyridyl ring (ring C) across the bridge. The H^6 protons of rings C and G are not directly over, or in the plane of, the ligand across the bridge and experience less anisotropy. The H^6 proton of ring G is in a slightly deshielding environment compared to the H^6 proton on ring C. The assignment of the two H^6 environments over the bridge in each diastereoisomer, in association with the connectivity discussed above, leads to the complete assignment of all the protons in these dinuclear complexes.

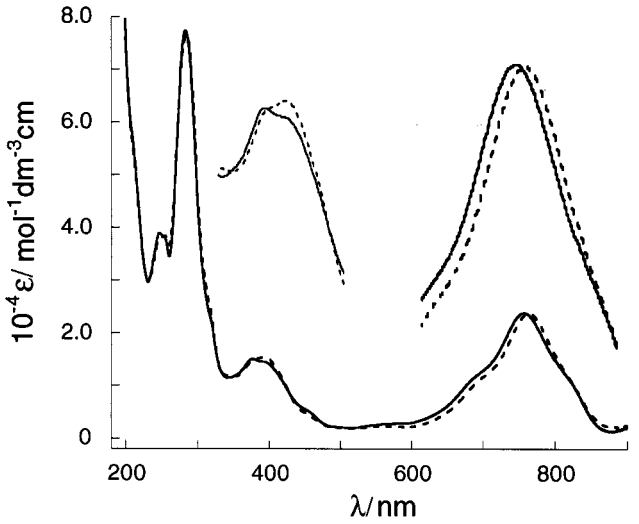

Figure 4. UV−visible absorption spectra (CH_3CN solution) of [{Ru(bpy)$_2$}$_2$(μ-apy)](PF$_6$)$_4$: *meso* (—); *rac* (- - -).

The ^{1}H-NMR analysis is consistent with the designation of the band 1 eluant as the *meso* isomer.

Electronic Spectroscopy. The absorption spectra of the complexes show intense bands in the UV region, with bands in the visible region (assigned as arising from MLCT transitions) at *ca.* 510 nm for the mononuclear species and at *ca.* 380 and 770 nm for the dinuclear compounds. As an example, the absorption spectra of the two diastereoisomers of [{Ru(bpy)$_2$}$_2$-(μ-apy)]$^{4+}$ are presented in Figure 4, and in the inset the expansion of the absorption arising from the lowest energy d(Ru) $\rightarrow \pi^*$(μ-apy) transition reveals a difference in MLCT energy between the two forms: i.e. there is a red shift of ~7 nm for the *rac* compared with the *meso* form. The stereochemistry also affects the d(Ru) $\rightarrow \pi^*$(bpy) transition; the shoulder at 400 nm for the *meso* isomers is enhanced for the *rac* isomers. For the complex [{Ru(bpy)$_2$}$_2$(μ-apy)]$^{4+}$ the λ_{max} is at 393 nm with the shoulder at 375 nm (see inset, Figure 4). We are not aware of other reports of a significant difference in such physical properties of ligand-bridged diastereoisomers. There have been numerous assertions that stereochemistry will have little influence on physical properties in circumstances where mixtures of isomers were investigated.[9,31] It is apparent now that the stereochemistry does influence the electronic transitions and the inter-metal communication.

The difference in spectral characteristics of the diastereoisomeric forms of these complexes might also be rationalized in terms of variations in solvation. Although the data are reported in acetonitrile solution, similar trends are observed in a number of solvents, which gives less credence to this alternative explanation. In any case, the differences still originate from stereochemical factors.

As well as the stereochemical influences on the electronic transitions, there are substituent effects. The shoulder at 400 nm discussed above is enhanced for dinuclear complexes with bpy compared to complexes containing Me$_2$bpy terminal ligands. Similarly, the shoulder at 830 nm is not present for complexes with the Me$_2$bpy terminal ligands. The dimers with the mapy bridge exhibit an additional shoulder at 420 nm.

The addition of methyl substituents to terminal polypyridyl ligands raises the energy of the d(Ru) orbital, lowering the d(Ru)

(31) Denti, G.; Campagna, S.; Serroni, S.; Ciano, M.; Balzani, V. *J. Am. Chem. Soc.* **1992**, *114*, 2944.

Table 2. Electronic Spectral and Electrochemical Data for Mono- and Dinuclear Ruthenium(II) Complexes in This Study (CH_3CN Solvent)

mononuclear complex	abs max λ, nm (log ϵ)	E_{MLCT},[a] eV	$\Delta E_{ox/red}$,[b] V
$[(bpy)_2Ru(apy)]^{2+}$	244 (4.36) 280 (4.61) 508 (3.88)	2.44	1.96
$[(Me_2bpy)_2Ru(apy)]^{2+}$	278 (4.67) 512 (3.93)	2.42	1.95
$[(bpy)_2Ru(mapy)]^{2+}$	246 (4.38) 280 (4.65) 506 (3.93)	2.45	1.97
$[(Me_2bpy)_2Ru(mapy)]^{2+}$	278 (4.65) 510 (3.92)	2.43	1.93

dinuclear complex		λ, nm (log ϵ)	E_{MLCT},[a] eV	$\Delta E_{ox/red}$,[b] V	ΔE_{ox},[c] V	log K_c[d]
$[\{Ru(bpy)_2\}_2(\mu\text{-apy})]^{4+}$	$\Delta\Lambda$	247 (4.59) 283 (4.89) 375 (4.18) 757 (4.38)	1.64	1.42	0.49	8.28
	$\Delta\Delta/\Lambda\Lambda$	255 (4.58) 284 (4.88) 393 (4.19) 764 (4.37)	1.62	1.44	0.50	8.45
$[\{Ru(Me_2bpy)_2\}_2(\mu\text{-apy})]^{4+}$	$\Delta\Lambda$	282 (4.94) 376 (4.25) 768 (4.41)	1.61	1.37	0.52	8.79
	$\Delta\Delta/\Lambda\Lambda$	283 (4.92) 380 (4.19) 775 (4.42)	1.60	1.40	0.53	8.96
$[\{Ru(bpy)_2\}_2(\mu\text{-mapy})]^{4+}$	$\Delta\Lambda$	246 (4.62) 283 (4.93) 377 (4.15) 761 (4.30)	1.63	1.42	0.47	7.95
	$\Delta\Delta/\Lambda\Lambda$	255 (4.60) 284 (4.92) 382 (4.15) 767 (4.32)	1.62	1.44	0.49	8.28
$[\{Ru(Me_2bpy)_2\}_2(\mu\text{-mapy})]^{4+}$	$\Delta\Lambda$	282 (4.92) 379 (4.11) 774 (4.35)	1.60	1.37	0.49	8.28
	$\Delta\Delta/\Lambda\Lambda$	283 (4.94) 383 (4.14) 778 (4.37)	1.59	1.39	0.51	8.62
$[(bpy)_2Ru(\mu\text{-mapy})Ru(Me_2bpy)_2]^{4+}$	$\Delta\Lambda/\Lambda\Delta$	255 (4.62) 283 (4.93) 378 (4.15) 766 (4.32)	1.62	1.39	0.50	8.45
	$\Delta\Delta/\Lambda\Lambda$	258 (4.60) 284 (4.92) 382 (4.12 773 (4.31)	1.60	1.41	0.52	8.79

[a] Energy for the lowest energy MLCT absorption. [b] Difference between the first oxidation and first reduction potential. [c] Difference between the first two oxidation potentials of the dinuclear complexes. [d] K_c is calculated comproportionation constant.

$\rightarrow \pi^*(\mu\text{-apy})$ MLCT energy.[32] The presence of methyl substituents on the bridge raises the π^* level. This is demonstrated by the bathochromic shift of the d(Ru) $\rightarrow \pi^*(\mu\text{-apy})$ transition in complexes containing methyl-substituted ligands (Table 2), as for each pair of methyl substituents (either on the bridge or on the terminal ligands) the MLCT absorption is red-shifted by 3 nm.

The large (250 nm) bathochromic shift upon coordination of a second $[Ru(bpy)_2]^{2+}$ moiety has been observed previously.[9] Methyl substituents on the terminal (bpy) or bridging (μ-apy) ligands increase such a shift by 6−15 nm as a result of the increased ligand σ-donor strength, the greatest effect being observed for $[\{Ru(Me_2bpy)_2\}_2(\mu\text{-mapy})]^{4+}$.

Electrochemistry. The redox couples in both the anodic and cathodic regions were determined for each mononuclear and dinuclear species using both cyclic voltammetry (CV) and differential pulse voltammetry (DPV) methods, the latter providing the greater precision and resolution. The close proximity to each other of the successive later ligand reductions rendered difficult the determination of some $E_{1/2}$ values from cyclic voltammetry. In these cases $E_{1/2}$ was calculated using the peak potential (E_p) from DPV, since

$$E_p = E_{1/2} - (PA)/2 \quad (1)$$

where PA is the pulse amplitude.[33]

For mononuclear complexes of the form $[Ru(pp)_2L]^{2+}$, all displayed one metal-centered oxidation ($Ru^{III/II}$) and four ligand reductions, each of which appeared to be a reversible redox process. Table 3 summarizes the electrochemical data obtained.

(32) Anderson, P. A.; Strouse, G. F.; Treadway, J. A.; Keene, F. R.; Meyer, T. J. *Inorg. Chem.* **1994**, *33*, 3863.
(33) Parry, E. P.; Osteryoung, R. A. *Anal. Chem.* **1965**, *37*, 1634.

Table 3. Redox Potentials (V vs Ag/Ag^+) for Mono- and Dinuclear Ruthenium(II) Complexes (CH_3CN/0.1 M $[(n\text{-}C_4H_9)_4N]ClO_4$ Solvent)[a]

	$E_{1/2ox(2)}$	$E_{1/2ox(1)}$	$E_{1/2red(1)}$	$E_{1/2red(2)}$	$E_{1/2red(3)}$	$E_{1/2red(4)}$	$E_{1/2red(5)}$	$E_{1/2red(6)}$
Mononuclear Complexes								
$[Ru(apy)(bpy)_2]^{2+}$	+1.29	−0.67	−1.38	−2.01	−2.37			
$[Ru(apy)(Me_2bpy)_2]^{2+}$	+1.22	−0.73	−1.44	−2.11	−2.42			
$[Ru(mapy)(bpy)_2]^{2+}$	+1.26	−0.71	−1.42	−2.02	−2.36			
$[Ru(mapy)(Me_2bpy)2]^{2+}$	+1.17	−0.76	−1.46	−2.11	−2.43			
Dinuclear Complexes								
ΔΛ-$[\{Ru(bpy)_2\}_2(\mu\text{-apy})]^{4+}$	+1.85	+1.36	−0.06	−0.71	−1.83[b]		−2.12	−2.23
ΔΔ/ΛΛ-$[\{Ru(bpy)_2\}_2(\mu\text{-apy})]^{4+}$	+1.87	+1.37	−0.07	−0.74	−1.84[b]		−2.15	−2.24
ΔΛ-$[\{Ru(Me_2bpy)_2\}_2(\mu\text{-apy})]^{4+}$	+1.75	+1.23	−0.15	−0.79	−1.94[b]		−2.21	−2.31
ΔΔ/ΛΛ-$[\{Ru(Me_2bpy)_2\}_2(\mu\text{-apy})]^{4+}$	+1.77	+1.24	−0.16	−0.82	−1.95[b]		−2.23	−2.33
ΔΛ-$[\{Ru(bpy)_2\}_2(\mu\text{-mapy})]^{4+}$	+1.78	+1.31	−0.11	−0.76	−1.85[b]		−2.14	−2.23
ΔΔ/ΛΛ-$[\{Ru(bpy)_2\}_2(\mu\text{-mapy})]^{4+}$	+1.82	+1.33	−0.11	−0.77	−1.84[b]		−2.16	−2.24
ΔΛ-$[\{Ru(Me_2bpy)_2\}_2(\mu\text{-mapy})]^{4+}$	+1.69	+1.20	−0.17	−0.82	−1.94[b]		−2.22	−2.32
ΔΔ/ΛΛ-$[\{Ru(Me_2bpy)_2\}_2(\mu\text{-mapy})]^{4+}$	+1.71	+1.20	−0.20	−0.85	−1.94[b]		−2.23	−2.34
ΔΛ/ΛΔ-$[(Me_2py)_2Ru(\mu\text{-mapy})Ru(bpy)_2]^{4+}$	+1.75	+1.25	−0.14	−0.79	−1.82	−1.95	−2.15	−2.29
ΔΔ/ΛΛ-$[(Me_2py)_2Ru(\mu\text{-mapy})Ru(bpy)_2]^{4+}$	+1.77	+1.25	−0.16	−0.82	−1.83	−1.95	−2.17	−2.32

[a] Calculated from DPV measurements (eq 1). [b] Two-electron reduction.

Table 4. Potential Differences ($\Delta E = E_{rac} - E_{meso}$) between the Diastereoisomeric Forms of the Dinuclear Species (mV vs Ag/Ag^+ Reference Electrode)[a]

dinuclear complex	$\Delta E_{ox(2)}$	$\Delta E_{ox(1)}$	$\Delta E_{red(1)}$	$\Delta E_{red(2)}$	$\Delta E_{red(3)}$	$\Delta E_{red(4)}$	$\Delta E_{red(5)}$	$\Delta E_{red(6)}$
$[\{Ru(bpy)_2\}_2(\mu\text{-apy})]^{4+}$	16	8	−12	−32	−4		−32	−12
$[\{Ru(Me_2bpy)_2\}_2(\mu\text{-apy})]^{4+}$	20	12	−12	−46	−8		−20	−24
$[\{Ru(bpy)_2\}_2(\mu\text{-mapy})]^{4+}$	40	24	4	−16	8		−20	−14
$[\{Ru(Me_2bpy)_2\}_2(\mu\text{-mapy})]^{4+}$	24	0	−24	−28	4		−16	−20
$[(bpy)_2Ru\{\mu\text{-mapy}\}Ru(Me_2bpy)_2]^{4+}$	20	0	−16	−24	−14	2	−18	−30

[a] Assessed from DPV measurements.

The bridging α-azodiimine ligands employed in this study are more π-accepting than the terminal ligands (bpy, Me_2bpy),[9,13] and consequently the first two electrons added to these complexes are localized on the α-azodiimine, as the second reduction process occurs at less cathodic potentials than any possible bpy-centered reduction. This has previously been confirmed using spectroelectrochemistry.[13]

The presence of methyl substituents on either the α-azodiimine or the bpy-type ligands affects the apy-centered reduction potentials. Conversely, methylation of apy ligand has no noticeable effect upon the bpy-centered reductions. The consequence of changing from bpy to Me_2bpy is to shift the two apy reductions ∼50 mV more cathodic, while the third and fourth redox couples move ∼100 mV. A comparison of the apy to the mapy complex shows ∼40 and ∼35 mV cathodic shifts (respectively) in only the first two couples. Since interchanging ligands also raises or lowers the d levels of the metal center, corresponding shifts in the oxidative $Ru^{III/II}$ couple are observed.

Previous studies have noted the correlation between $\Delta E_{ox/red}$ (the potential difference between the couples associated with the metal-based oxidation and the first ligand-based reduction—and therefore between the HOMO and LUMO energy levels) and E_{MLCT} (the energy associated with the lowest MLCT absorption) for a selection of tris(bidentate)ruthenium(II) complexes containing polypyridyl ligands.[34−36] There are some notable exceptions, including complexes containing the ligand dipyrido[3,2-*c*:2′,3′-*e*]pyridazine (taphen),[37,38] where it has been suggested the reduction involves population of the LUMO (π_1*) level while the MLCT absorption involves a transition to the SLUMO(π_2*). It is noted in passing that the present mononuclear complexes of apy and mapy do not correlate with the general trend either: a plot of $\Delta E_{ox/red}$ vs E_{MLCT} for a variety of tris(bidentate)ruthenium(II) complexes and for the mononuclear species in the present study are given as Supporting Information (Figure S3).

For dinuclear complexes of the form $[(pp)_2Ru(\mu\text{-L})Ru(pp)_2]^{4+}$, two widely separated metal-centered oxidations and five (six in the case of the "mixed-end" dimer) ligand-based reductions were observed, all of which appeared to be reversible redox couples. Previous studies undertaken in a different solvent[13] identified a sixth couple at more negative potentials for the $[\{Ru(bpy)_2\}_2(\mu\text{-apy})]^{4+}$ complex: the present investigation was undertaken using CH_3CN/0.1 M $[(n\text{-}C_4H_9)_4N]ClO_4$, which imposes a reductive limit of ∼−2500 mV (vs Ag/Ag^+), but it is reasonable to predict the existence of an analogous couple at more negative potentials for the other dinuclear species studied.

One of the significant aspects of this work is that, having separated the diastereoisomeric pairs for each of the five dinuclear complexes synthesized, we observed measurable differences in the physical properties not only between the different complexes but also between the two diastereoisomers of the same complex. The net differences between the *rac* and the *meso* forms for each redox couple of the various dinuclear species are summarized in Table 4. In all the complexes, the oxidative couples are shifted to more positive potentials and the reductive couples to more negative potentials for the *rac* (ΔΔ/ΛΛ) forms relative to the *meso* (ΔΛ) diastereoisomers. Additionally, the separation between the two metal-centered oxidations ($\Delta E_{1/2ox}$) is consistently larger for the *rac* form. This implies a slightly greater degree of metal−metal communication for one stereochemical form over the other (the comproportionation constants are given in Table 2), and we believe this to be the first observation of stereochemical influences on the electron transfer properties within dinuclear metallic complexes.

(34) Dodsworth, E. S.; Lever, A. B. P. *Chem. Phys. Lett.* **1985**, *119*, 61.
(35) Dodsworth, E. S.; Lever, A. B. P. *Chem. Phys. Lett.* **1986**, *120*, 152.
(36) Juris, A.; Barigelletti, S.; Campagna, S.; Balzani, V.; Belser, P.; von Zelewsky, A. *Coord. Chem. Rev.* **1988**, *84*, 85.
(37) Juris, A.; Belser, P.; Barigelletti, F.; von Zelewsky, A.; Balzani, V. *Inorg. Chem.* **1986**, *25*, 256.
(38) Barigelletti, F.; Juris, A.; Balzani, V.; Belser, P.; von Zelewsky, A. *Inorg. Chem.* **1987**, *26*, 4115.

Scheme 1

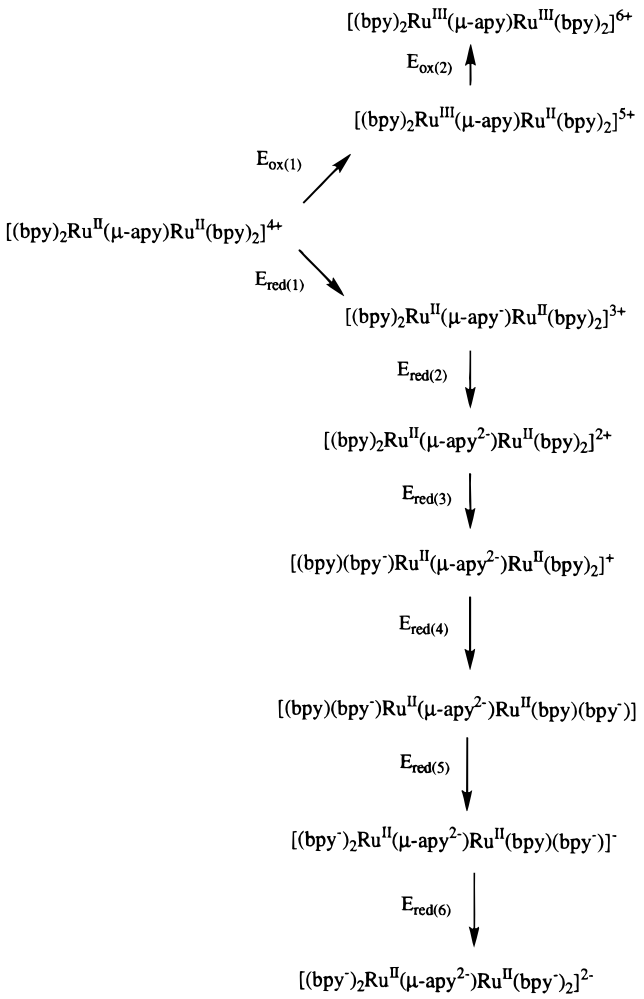

Earlier work,[9,13] which exclusively studied the $[\{Ru(bpy)_2\}_2(\mu\text{-apy})]^{4+}$ dinuclear species in DMF solution, tentatively assigned the first two reductions as bridge-centered and the next two-electron process as bpy-centered. This was then said to be followed by three further two-electron processes, the first of these again bridge-centered and the other two bpy-centered. This suggested the possibility of achieving the reversible acceptance of 10 electrons by the dinuclear complex. With the advantage of having prepared and measured a larger number of dinuclear α-azodiimine species in the present work, we prefer alternative assignments for the redox couples labeled $E_{1/2red(5)}$ and $E_{1/2red(6)}$, shown in Scheme 1, on the basis of our studies in acetonitrile solution.

The effect on the redox couples of a methyl substituent at the bridge or the peripheral ligands follows the trends observed for the mononuclear complexes. Comparison of the apy- to the mapy-bridged complexes reveals a ~40 mV and a ~30 mV cathodic shift (respectively) for the first two bridge-centered reductions. The same couples are cathodically shifted ~85 mV when methyl substituents are added to the four terminal ligands. Smaller shifts (only 50 mV) were observed for the mononuclear species, which is consistent in simplistic additive terms; i.e., there are twice as many nonbridging ligands in the dinuclear species compared with the corresponding mononuclear case. This is confirmed by examining $[(bpy)_2Ru(\mu\text{-mapy})Ru(Me_2bpy)_2]^{4+}$—the so-called "mixed-end" dimer—where the shift is ~35 mV: here Me_2bpy ligands are coordinated to only one of the two ruthenium centers.

Figure 5 shows differential pulse voltammograms of the *rac* diastereoisomers of three dimer species bridged by mapy. When

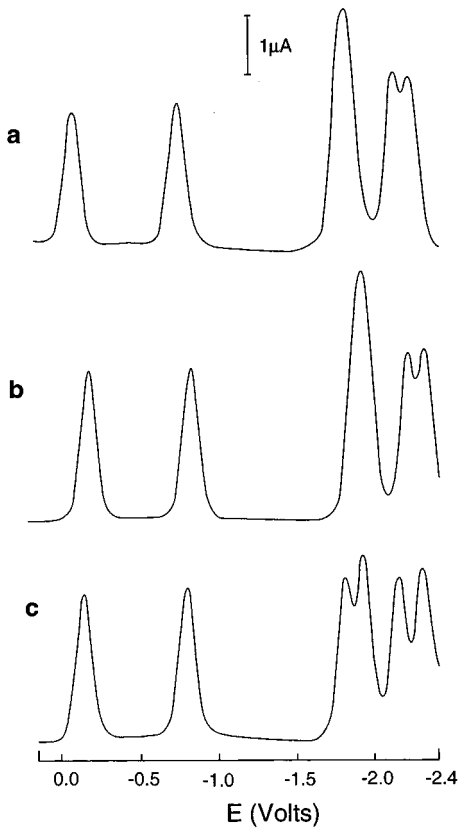

Figure 5. Differential pulse voltammograms for the *rac* (ΔΔ/ΛΛ) forms of (a) $[\{Ru(bpy)_2\}_2(\mu\text{-mapy})]^{4+}$, (b) $[\{Ru(Me_2bpy)_2\}_2(\mu\text{-mapy})]^{4+}$, and (c) $[(bpy)_2Ru(\mu\text{-mapy})Ru(Me_2bpy)_2]^{4+}$ (CH_3CN/0.1 M $[(n\text{-}C_4H_9)_4N]ClO_4$ solution; Pt working electrode; Ag/Ag^+ reference electrode).

the terminal ligands attached to both ruthenium centers in the dimer are the same, there is a broad peak ($E_{1/2red(3)}$) associated with a two-electron process (or more probably, two one-electron reductions occurring almost simultaneously at opposite ends of the molecule). For the "mixed-end" dimer (Figure 5c), there are two distinctly resolved one-electron peaks, now separated by over 100 mV. By comparison with responses shown in Figures 5a,b, the first peak can be assigned as a reduction of a bpy ligand attached to one metal center, and the second ($E_{1/2red(4)}$), as a reduction of Me_2bpy attached to the other metal. These $E_{1/2}$ values (Table 4) are consistent with those of the symmetrical dimers in which the terminal ligands are all bpy and all Me_2bpy, respectively. As with the mononuclear species, the presence of methyl substituents on the α-azodiimine bridge does not appear to affect the reduction potentials of the terminal (non-bridging) ligands.

The redox couple labeled $E_{1/2red(5)}$ was previously assigned as a two-electron bridge-centered reduction[13] for the complex $[\{Ru(bpy)_2\}_2(\mu\text{-apy})]^{4+}$. After integration of the area under the DPV response for this compound and also the four other α-azodiimine-bridged species, it now appears to be a single-electron, bpy-centered process. Similarly, $E_{1/2red(6)}$, which was also thought to involve two electrons, now appears to be a single-electron reduction. The original assignment of $E_{1/2red(5)}$ was based upon spectroelectrochemical studies and the presence of nonreduced bpy in the spectrum of what was assumed to be the $[\{Ru(bpy)_2\}_2(\mu\text{-apy})]^{2-}$ anion. This implied the presence of a $\{\mu\text{-apy}\}^{4-}$ moiety, although characteristic absorption features for this ligand could not be established. However if $E_{1/2red(5)}$ involves only a single electron transfer, then the anion investigated was actually $[\{Ru(bpy)_2\}_2(\mu\text{-apy})]^{-}$, which would still possess an unreduced terminal ligand. An examination of the redox potentials shows shifts of ~85 mV for these couples

between the species containing bpy and Me_2bpy as terminal ligands. Modification of the bridging ligand by methyl substitution has no effect on either the fifth or sixth reductions. If $E_{1/2red(5)}$ was bridge-centered, the electron-donating ability of a methyl substitutent would be expected to make reduction more difficult, and by analogy to the case of $E_{1/2red(1)}$ and $E_{1/2red(2)}$ (which are indeed bridge-based processes) a cathodic shift of ~35 mV might be anticipated.

Spectroelectrochemisty. Spectroelectrochemical studies of the dinuclear complexes show isosbestic points for the first oxidation process and for the first two reductions. The full oxidation of both metal centers to the trivalent state could not be achieved at −32 °C due to the electrochemical limits of the solvent ($[(n\text{-}C_4H_9)_4N]ClO_4$ in acetonitrile). Reversibility of the first oxidation and the six reduction steps was demonstrated by the coincidence of the isosbestic points during each reverse electrolysis step and ultimate recovery of the starting compound.

The first oxidation is a one-electron process producing the mixed-valence species $[(pp)_2Ru^{III}(\mu\text{-L})Ru^{II}(pp)_2]^{5+}$, which have IVCT bands (ν_{max} 6800−6900 cm^{-1}; ϵ_{max} 800−1200 mol^{-1} dm^3 cm^{-1}; $\Delta\nu_{1/2}$ 1600−1900 cm^{-1}). The formation of these IVCT bands in a spectroelectrochemical experiment is shown for the oxidation of *meso*-$[(bpy)_2Ru^{II}(\mu\text{-mapy})Ru^{II}(bpy)_2]^{4+}$ in Figure S4 (Supporting Information). There is a small difference in the shape of the IVCT band between the two compounds $[(bpy)_2Ru^{III}(\mu\text{-mapy})Ru^{II}(bpy)_2]^{5+}$ and $[(Me_2bpy)_2Ru^{III}(\mu\text{-mapy})Ru^{II}(Me_2bpy)_2]^{5+}$. However, there is no discernible difference between diastereoisomers of the same species. The difference in communication between the metal centers observed in electrochemical measurements of the $[(bpy)_2Ru^{III}(\mu\text{-mapy})Ru^{II}(bpy)_2]^{5+}$ diastereoisomers ($E_{1/2ox}$) did not manifest itself in any detectable variation between the IVCT bands, the two band shapes (including $\Delta\nu_{1/2}$) appearing almost superimposable.

These mixed-valent dinuclear species containing the α-azodiimine bridging ligands have previously been categorized as both weakly interacting (class II)[7] and strongly interacting (class III)[39] systems, and the complexes do not clearly meet the criteria for either assignment. In the application of Hush's theory[40,41] to the IVCT band, a large discepancy is observed between the calculated $\Delta\nu_{1/2}$ and the experimental value. While a strong solvent dependency may account for this (our measurements were only carried out in a single solvent), the nonapplicability of the theory suggests a large degree of delocalization and thus strongly interacting (class III) behavior.[7,39,42]

The spectroelectrochemistry studies of the six reduction steps in the dinuclear species support our previous assertions that the first two reductions are centered on the bridge and the next four one-electron reductions are localized on the terminal ligands. The spectral changes associated with the first two reduction processes can be seen in Figure 6, where they are shown as the reverse oxidations [2+] → [3+] and [3+] → [4+]. In the first reduction, the d(Ru) → π^*(bpy) MLCT absorption is red-shifted and the d(Ru) → π^*(bridge) MLCT absorption undergoes a blue shift, consistent with the first electron being localized on the azobis(4-methyl-2-pyridine) bridge. The red shift is the smaller electronic effect, as bridge reduction raises the d(Ru) level. The band attributed to the d(Ru) → π^*(bridge) MLCT absorption collapses completely upon addition of the second electron, while the d(Ru) → π^*(bpy) MLCT absorption is further red-shifted, confirming that this second electron is also localized on the bridge.

(39) Crutchley, R. J. *Adv. Inorg. Chem.* **1994**, *41*, 273.
(40) Hush, N. S. *Prog. Inorg. Chem.* **1967**, *8*, 391.
(41) Allen, G. C.; Hush, N. S. *Prog. Inorg. Chem.* **1967**, *8*, 357.
(42) Poppe, J.; Moscherosch, M.; Kaim, W. *Inorg. Chem.* **1993**, *32*, 2640.

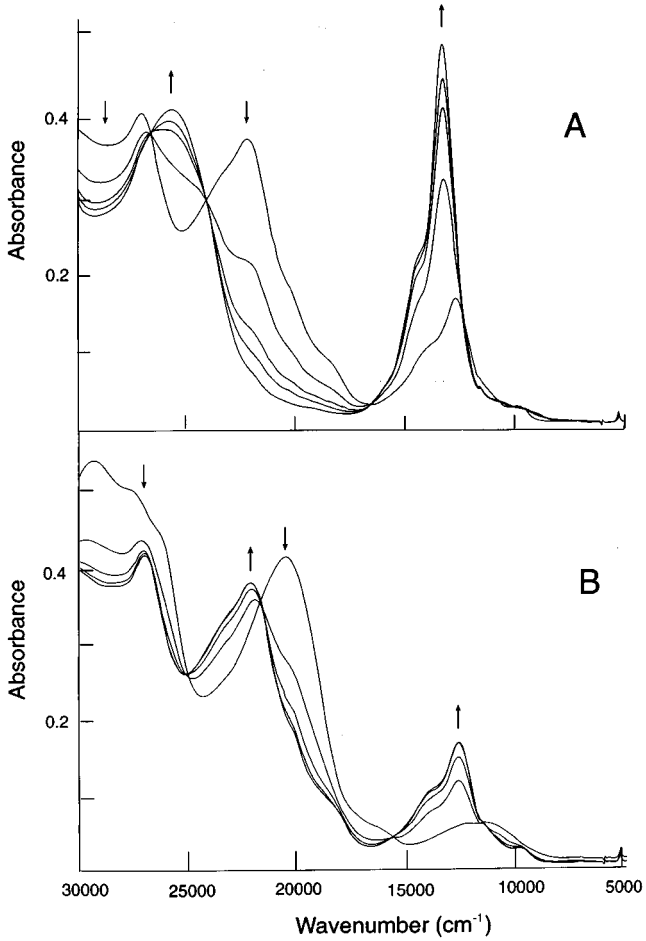

Figure 6. Spectroelectrochemical changes for the oxidation reactions (A) *meso*-$[(bpy)_2Ru^{II}(\mu\text{-mapy}^-)Ru^{II}(bpy)_2]^{3+}$ → *meso*-$[(bpy)_2Ru^{II}(\mu\text{-mapy})Ru^{II}(bpy)_2]^{4+}$ and (B) *meso*-$[(bpy)_2Ru^{II}(\mu\text{-mapy}^{2-})Ru^{II}(bpy)_2]^{2+}$ → *meso*-$[(bpy)_2Ru^{II}(\mu\text{-mapy}^-)Ru^{II}(bpy)_2]^{3+}$ (CH_3CN/0.1 M $[(n\text{-}C_4H_9)_4N]ClO_4$ solution).

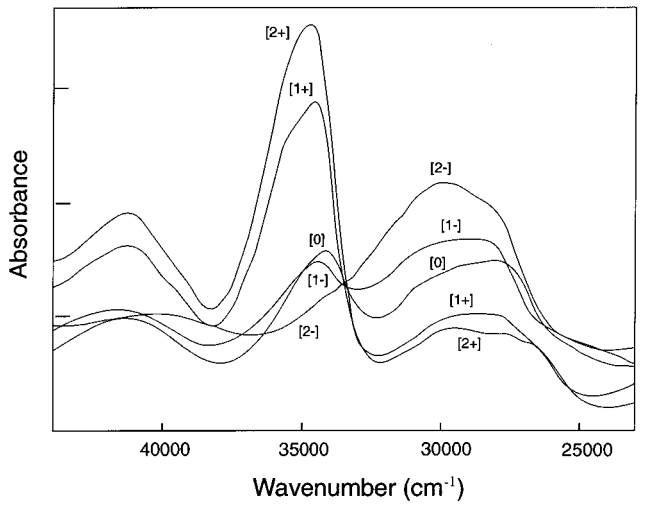

Figure 7. UV−visible absorption spectra (acetonitrile solution) of *meso*-$[(bpy)_2Ru(\mu\text{-mapy})Ru(bpy)_2]^{n+}$: [2+], $[(bpy)_2Ru^{II}(\mu\text{-mapy}^{2-})Ru^{II}(bpy)_2]^{2+}$; [1+], $[(bpy^-)(bpy)Ru^{II}(\mu\text{-mapy}^{2-})Ru^{II}(bpy)_2]^{+}$; [0], $[(bpy^-)(bpy)Ru^{II}(\mu\text{-mapy}^{2-})Ru^{II}(bpy)(bpy^-)]$; [1−], $[(bpy^-)_2Ru^{II}(\mu\text{-mapy}^{2-})Ru^{II}(bpy)(bpy^-)]^-$; [2−], $[(bpy^-)_2Ru^{II}(\mu\text{-mapy}^{2-})Ru^{II}(bpy^-)_2]^{2-}$.

The bpy^0 and bpy^- bands located in the UV region (centered at 33 800 and 29 600 cm^{-1} respectively; Figure 7) demonstrate that the next four one-electron reductions are localized sequentially on each of the terminal bpy ligands. For each successive reduction ($E_{1/2red(3-6)}$) the bpy^0 band decreases in intensity and

finally collapses completely, while the bpy^- band correspondingly increases with each reductive step.

Conclusions

The synthesis of a series of α-azodiimine-bridged diruthenium(II) species and their separation in each case into diastereoisomers have permitted the observation and measurement of physical differences between the *meso* and *racemic* forms. Comparisons of the electronic spectra of the two diastereoisomeric forms show a ∼6 nm difference in the MLCT absorptions. Electrochemical studies reveal anodic shifts for oxidative couples and cathodic shifts for reductive couples of 0−45 mV for the *racemic* relative to the *meso* forms of each of the five dinuclear complexes investigated. Similarly, there are differences in the comproportionation constants between diastereoisomeric forms as calculated from the $E_{1/2redox}$ measurements, although no discernible differences were observed between the IVCT bands of the respective forms. Significant structural differences in the relative orientations of the terminal ligands are reflected electronically in the markedly different ^{1}H-NMR spectra. The *meso* forms always appear as the major product from the synthesis and have a much lower solubility in a wide range of organic solvents.

The first six electrochemical reductions for this series of dinuclear complexes have been unequivocally assigned. Contrary to a previous report in the literature, there are six one-electron steps—the first two are centered on the bridge and the following four localized on the four terminal ligands.

Acknowledgment. This work was supported by the Australian Research Council. We are grateful to Dr. Graham Heath for the use of the OTTLE cell facilities at the Australian National University.

Supporting Information Available: Figures S1−S4, showing CHEM 3D representations of the diastereoisomeric forms of $[\{Ru(Me_2bpy)_2\}_2(\mu\text{-apy})]^{4+}$, portions of the 300 MHz ^{1}H-NMR NOE difference spectra of *rac*-$[\{Ru(Me_2bpy)_2\}_2(\mu\text{-mapy})]^{4+}$, correlation between $\Delta E_{ox/red}$ (potential difference between the first oxidation and first reduction processes) and E_{MLCT} (the lowest energy MLCT absorption) for tris(bidentate)ruthenium complexes containing polypyridyl ligands, and spectroelectrochemical changes for the oxidation reaction *meso*-$[(bpy)_2Ru^{II}(\mu\text{-mapy})Ru^{II}(bpy)_2]^{4+} \rightarrow$ *meso*-$[(bpy)_2Ru^{III}(\mu\text{-mapy})Ru^{II}(bpy)_2]^{5+}$ (CH_3CN/0.1 M $[(n\text{-}C_4H_9)_4N]ClO_4$ solution), and an Appendix giving the data used to generate Figure S3 (5 pages). Ordering information is given on any current masthead page.

IC9600893